Effect of Pressure on Hydrodynamic Parameters of Several PTR Regenerator Fillers in Axial Steady Flow

E.C. Landrum[1], T.J. Conrad[1], S.M. Ghiaasiaan[1] and C.S. Kirkconnell[2]

[1]Georgia Institute of Technology, Atlanta, GA 30332
[2]Raytheon Space and Airborne Systems, El Segundo, CA 90245

ABSTRACT

An experimental investigation was carried out to measure the effect of average pressure on the porous media hydrodynamic closure relations relevant to steady axial flow through several regenerator fillers. Using room temperature helium as the working fluid, pressure drops occurring across a test section that contained various regenerator filler materials were measured. The test apparatus allowed for the adjustment of the mean pressure in the test section. The tested regenerator samples included stacked screens of stainless steel mesh 325 and stainless steel 400 mesh, screens of stainless steel 400 mesh stacked and sintered together and a stainless steel metal foam. The helium superficial velocity (Darcy velocity) through the porous samples covered a range from 0.2 to 19 m/s. The test section and its vicinity were then modeled as a porous structure using the Fluent CFD code, and the model porous media hydrodynamic parameters were iteratively adjusted to match the model predictions to the experimental results. Using this methodology, it was possible to determine axial viscous and inertial resistances related to the Darcy permeability and Forchheimer inertial coefficient, respectively, for all the porous samples. The results are tabulated for the investigated porous media and indicate that the axial hydrodynamic parameters are insensitive to the test section average pressure, provided that the pressure drop through the porous sample is limited to about 0.7 MPa (100 psi).

INTRODUCTION

Computational fluid dynamics (CFD) modeling is possibly the best available technique in designing and predicting the performance of cryocoolers. Pulse tube cryocoolers function with micro porous material housed within their regenerator and heat exchanger components; however, the thermal and hydrodynamic transport phenomena associated with these micro structures are not fully understood. Complete analysis of the fluid-solid interaction through this media can be obtained only by direct pore level simulation[1], a method which is time consuming and impractical for system level examinations.

Navier-Stokes and energy equations can be volume averaged, leading to conservation equations which capture the macroscopic fluid behavior in porous media without solving for the detailed fluid motion at the microscopic scale. These porous media equations require empirical closure relations. Constitutive relationships, such as the Darcy permeability and Forchheimer's inertial coefficient, are needed for the closure of these macroscopic volume-averaged conservation

Cryocoolers 15, edited by S.D. Miller and R.G. Ross, Jr.

equations.[2] Generally, porous media of interest for cryocoolers are morphologically anisotropic therefore the parameters which characterize them depend on the filler type as well as flow direction. In this work, steady flow hydrodynamic parameters are determined using an experimentally measured relationship between fluid flow rate and the pressure drop across the porous media representing several regenerator fillers. Simulating the experimental test sections in CFD, we can iteratively adjust the viscous and inertial flow resistances until agreement is reached between simulated and experimental results.

This paper reports on a study of the effect of average fluid pressure on the hydrodynamic parameters associated with steady state axial flow through four regenerator fillers. A previous investigation[3] indicated that the values of these parameters might be sensitive to the average fluid pressure in a porous sample. The previous results were not conclusive, however, as large variations in average pressure were allowed in the tests. The four types of porous material investigated here include a 325 mesh stainless steel wire cloth, a 400 mesh stainless steel wire cloth, a 400 mesh stainless steel sintered wire cloth and a stainless steel metal foam. All test samples are common fillers of cryocooler regenerators. In the following sections, the experimental and computational methodologies employed in solving for steady axial flow hydrodynamic resistances are first discussed. The experimental data for each filler sample at three distinct operating pressures is then presented and discussed.

EXPERIMENTAL SETUP

The experimental setup utilized in determining the hydrodynamic steady axial flow resistance parameters consisted of a helium supply tank and pressure regulator, two Paine Electronics low pressure series 210-10 static pressure transducers, a Sierra Instruments 820 Series Top-Trak mass flow meter, a specially designed test section containing the porous sample and the associated piping and Swagelok® fittings and valves. Each pressure signal was amplified and calibrated through using an Omega DMD-465WB signal conditioner. The static pressure transducers and mass flow meter have an accuracy of ±0.25% and ±1.5% of full scale, respectively. Pressure and mass flow rate measurements were read as analogue voltage signals via hand held digital multimeters. This setup and procedure is similar to what was employed earlier by Clearman[3] and Cha.[1] A diagram of the setup is shown in Figure 1.

The axial test section which houses the porous media is a hollow aluminum cylinder with an inner diameter of 0.3125 in (7.94 mm). End pieces bolted onto flanges located on either side of the test section constrain the porous samples and provide a mount for one of the static pressure transducers. Valves, V1 and V2, and the static pressure transducers, P1 and P2, are respectively located upstream and downstream of the test section.

The test sample and housing were specifically designed with a large aspect ratio of 4.8 to ensure the flow had a predominant velocity component in the axial direction; therefore flow in the radial direction can be considered to be small. Each porous sample was fabricated with strict tolerances to have negligible clearance between its circumference and the inside of the test section housing. The 400 mesh sintered cloth and metal foam samples were supplied by Raytheon. A wire

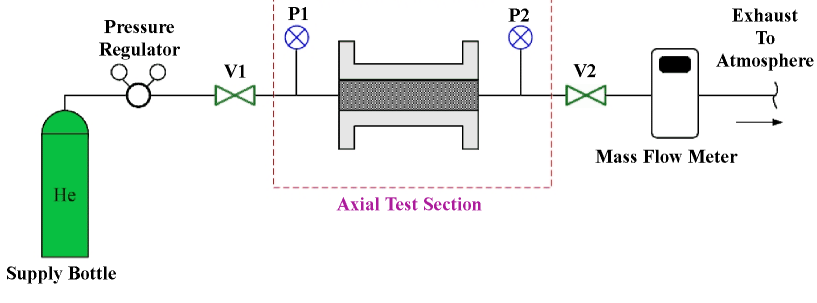

Figure 1. Experimental setup.

electrical discharge machining technique was exercised in manufacturing the sintered and metal foam samples while a punching operation was applied to the other mesh samples. All mesh samples consisted of a plain square weave pattern with uniform pore size. The 400 and 325 mesh cloths were cut into disks and stacked within the container while the 400 mesh sintered sample was cut and thermally bonded into three separate pieces which were then loaded into the sample housing. The metal foam was also constructed through a sintering process and cut into a single cylinder which could be inserted. Important details of each test piece including wire diameter, pore size and sample porosity are summarized in Table 1. Sample porosity was determined by using the sample's mass, material density and total occupied volume. Wire diameter and pore size were specified by the vendor.

During each steady axial flow test, research grade helium with a nominal purity of 99.9999% flows from the charged bottle through the pressure regulator, past the valve V1 and into the axial test section. Helium then leaves the test section through valve V2 and is straightened in a long tube before it passes through the mass flow meter, after which it is exhausted to the atmosphere. The mass flow meter was calibrated at atmospheric conditions and is consequently located just before the exhaust. Each test run was performed only after strict assurance of a hermetically sealed setup. With valve V2 closed and valve V1 open, the isolated system was charged to a predetermined supply pressure. Axial pressure tests for each porous sample were performed at three different supply pressures; 300 psig (2.07 MPa), 400 psig (2.76 MPa) and at the regulator's nominal maximum pressure of 500 psig (3.45 MPa). Valve V2 was then modulated to offer a range of mass flow rates up to 1.67 g/s. Static pressures P1 and P2 were recorded for each distinct mass flow rate. As valve V2 is opened, the downstream pressure P2 decreases and thus the average pressure inside the porous structure decreases as the mass flow rate increases. In order to avoid large variations in the mean pressure during experiments with each sample, the maximum axial pressure drop across the test section was constrained to 100 psi (0.69 MPa). Therefore, the average pressure in the test section can deviate no more than 50 psi during any test run. In the results described below, all of the data are reported with a nominal mean pressure, namely the supply pressure set by the regulator. All test runs are performed at room temperature 75° F (24° C) where the working fluid is considered isothermal and the viscosity is assumed to be a constant.

As mentioned earlier, the momentum closure parameters for steady flow are determined by the correlation between pressure drop and flow rate. For each test run, axial pressure drops between static pressures measurement locations P1 and P2 were then plotted as a function of mass flow rate. Experimental datum for each test sample at each supply pressure is curved fitted to a 5^{th} order polynomial with a zero intercept, and the developed polynomial was then utilized in order to simplify the data analysis. Plots of experimental data can be seen in Figs. 2, 3, 4 and 5.

CFD ASSISTED METHODOLOGY

CFD analysis is a useful method that enables us to iteratively determine the hydrodynamic viscous and inertial resistances in the experiments. The CFD simulations were performed with the commercially available Fluent software package. Our Fluent model utilizes basic continuum based conservation equations governing single phase fluid flow in open and porous media. The advantage of CFD analysis is that the numerical solution method provides a rigorous account of the macroscopic flow phenomena without making any arbitrary simplifying assumptions.[1]

Based upon the experimental curve fit polynomials for each sample's discrete supply pres-

Table 1. Steady axial flow test sample details.

	Sample Geometry		Mesh Geometry		Measured
Porous Media	Dia mm	Length mm	Wire Dia mm	Pore Size micron	Porosity ---
325 Stainless Steel	7.938	38.1	35.6	43	0.6738
400 Stainless Steel	7.938	38.1	25.4	33	0.6312
400 Stainless Steel (Sintered)	7.938	38.1	25.4	-	0.6312
Stainless Steel Foam	7.938	38.1	-	-	0.5547

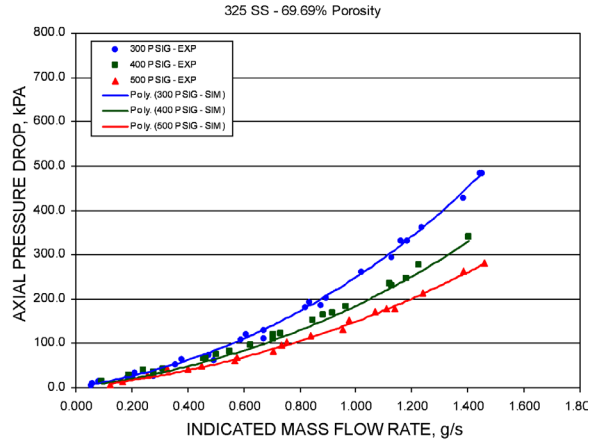

Figure 2. Axial pressure drops for 325 stainless steel test sample.

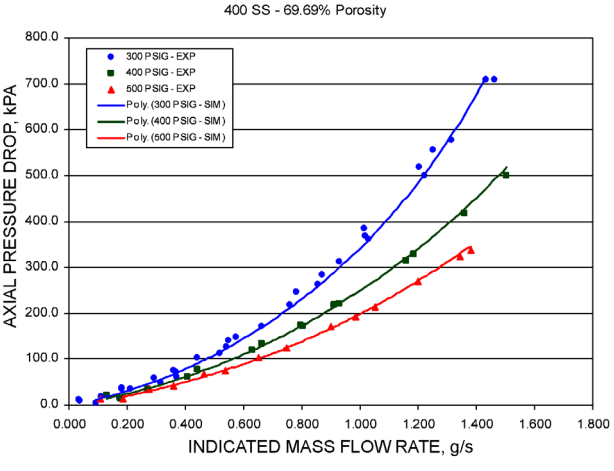

Figure 3. Axial pressure drops for 400 stainless steel test sample.

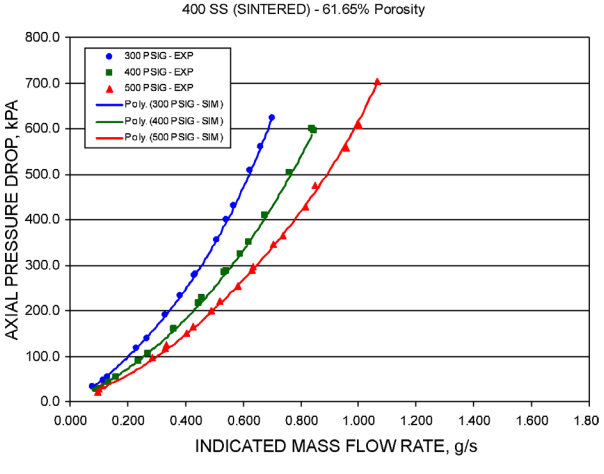

Figure 4. Axial pressure drops for 400 stainless steel sintered test sample.

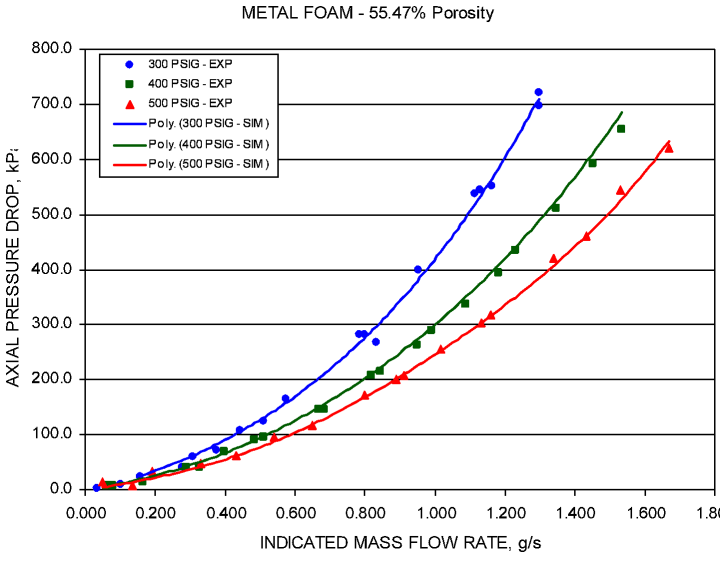

Figure 5. Axial pressure drops for stainless steel metal foam test sample.

sures, seven representative experimental data points were chosen from the full range of mass flow rates, and were then input to the CFD code. A single Fluent case was created for each of the seven representative data points with its own unique pressure drop and mass flow rate. The simulations used a 2-D axisymmetric mesh that modeled the laminar flow within the experimental test setup between static pressure transducers, P1 and P2. Several nodal networks of various nodal spacing were developed to examine the effects of mesh size on the simulation outcome. Eventually, a grid system with an average nodal spacing of 0.015 in (0.38 mm) in the radial direction and 0.03 in (0.76 mm) in the axial direction was used in each case. With this nodal spacing the simulation results were reasonably insensitive to further reduction in nodal size, while the computational time was affordable.

In each simulation, the relevant experimentally measured values were introduced as the boundary conditions. A mass flow rate boundary condition was implemented at P1, the inlet to the simulated segment of the test apparatus, while a pressure outlet boundary condition was applied at the P2 location. The model's viscous and inertial resistances were iteratively changed until there was agreement between the predicted area-weighted static pressure at the inlet and experimental static pressure at P1. The viscous resistance could be determined at low flow rates where the inertial effects could be considered negligible. A trial and error method was used until a unique viscous resistance satisfied the first several data points of the low flow regime. This term was then fixed and only the inertial resistance was adjusted for the other data points. The iterative solution process was continued until good agreement was achieved between simulated and experimental pressure drops across the entire range of mass flow rates.

RESULTS

Fluent simulations were done for all four porous structures at each of the three supply pressures of 2.07, 2.76 and 3.45 MPa. The viscous and inertial resistances were first determined at the supply pressure which presented the greatest range of axial pressure drops and mass flow rates. These parameters were then applied to the data representing the other two supply pressures. The 2.07 MPa (300 psig) supply pressure was suitable for the initial determination of flow parameters for the high-porosity materials such as the 325 and 400 mesh samples, whereas the maximum supply pressure of 3.45 MPa (500 psig) offered the largest range of pressure drop and mass flow rate variations for more resistive materials like the 400 sintered mesh and metal foam.

Figs. 2 through 5 display the axial pressure drops versus mass flow rate for the four tested regenerator samples. Discrete experimental data points as well as the aforementioned 5th order polynomials are shown in the figures. Mass flow rates ranged from 0.032 g/s to 1.668 g/s with pressure drops across the test section limited to 100 psi (0.69 MPa). Multiple tests were performed for each filler and the results were found to be well repeatable.

As mentioned earlier, the design of the test apparatus was expected to render the flow in the porous test section primarily one-dimensional, in the axial direction. The CFD simulations have shown that this was indeed the case. The velocity vectors are displayed in Fig. 6 for a typical case. The figure shows the velocity vectors in the porous test section for the sintered stainless steel 400 mesh filler type at a mass flow rate of 0.84 g/s. The flow is evidently predominately axial, except for the immediate vicinity of the flow area change near the exit from the porous segment where two-dimensional flow effects are noticeable.

The vector form of the volume-average momentum equation of fluid within the porous structure is shown in Eq. (1).

$$\frac{\partial}{\partial t}\left(\varepsilon\rho\vec{u}\right)+\nabla\cdot\left(\varepsilon\rho\vec{u}\vec{u}\right)+\varepsilon\nabla P+\nabla\cdot\left(\varepsilon\bar{\bar{\tau}}\right)-\varepsilon\vec{F}_{bf}+\mu\bar{\bar{D}}\cdot\vec{u}+\frac{\bar{\bar{C}}\rho}{2}\cdot\left|\vec{u}\right|\vec{u}=0 \tag{1}$$

The sample porosity is represented by ε while the viscous and inertial resistance coefficient tensors are $\bar{\bar{D}}$ and $\bar{\bar{C}}$ units of 1/m^2 and 1/m, respectively. Fluid density and viscosity are displayed as ρ and μ, and $\bar{\bar{\tau}}$ represents the stress tensor. Thermodynamic pressure is shown with P and $\vec{F}_{bf}$ represents the body force vectors (our particular simulations do not include any body forces or gravity). The vector u represents the physical velocity within the porous structure. Assuming isotropic flow resistances, one can equate the last two terms in Eq. (1) to constant scalar values on the right side of Eq. (2) which include the Darcy permeability, K and Forchheimer's inertial coefficient, c_f. This relationship between isotropic resistance tensors, Darcy permeability and Forchheimer's inertial coefficient is shown directly in Eqs. (3) and (4).

$$\mu D\vec{u}+\frac{C\rho}{2}\left|\vec{u}\right|\vec{u}=\frac{\varepsilon^2\mu}{K}\vec{u}+\frac{c_f\varepsilon^3\rho}{\sqrt{K}}\left|\vec{u}\right|\vec{u} \tag{2}$$

$$K=\varepsilon^2/D \tag{3}$$

$$c_f=\frac{C\sqrt{K}}{2\varepsilon^3} \tag{4}$$

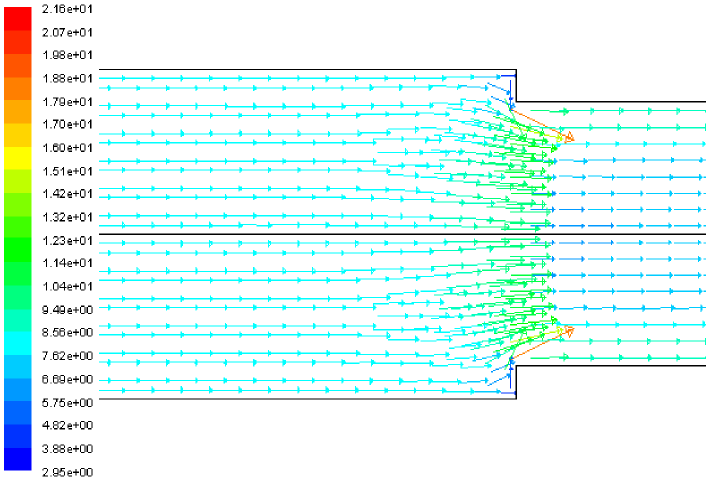

Figure 6. Velocity vectors colored by magnitude (m/s) in the porous section at 0.84 g/s, for the sintered stainless steel 400 mesh filler at 61.65% porosity.

The assumption of isotropy is, of course unrealistic, but is justifiable here because the flow in the test section is predominantly axial, and CFD simulations show that the results are insensitive to the magnitude of the flow resistance parameters in the radial direction.

Despite the differences in the flow rate to pressure drop curves for the different supply pressures, a single set of hydrodynamic parameters for each porous structure resulted in good agreement between experimental and simulated data for all test runs at all three supply pressures. These hydrodynamic parameters are summarized in Table 2.

The insensitivity of the hydrodynamic parameters to the mean pressure is in contrast to the observation reported in a previous investigation[3], where steady axial flow resistances were determined for a single regenerative filler at four distinct supply pressures; 300 psig (2.07 MPa), 350 psig (2.41 MPa), 400 psig (2.76 MPa), and 500 psig (3.45 MPa). A review of the data, however, indicates that the experimental data involved large pressure drops, in the range of 13.8 to 2113 kPa across their test section with fluctuations in average pressure of nearly 1230 kPa. Without a fine limit on the change in pressure, it difficult to categorize porous hydrodynamic parameters based upon average pressure. These large pressure variations evidently make it difficult to unambiguously separate the frictional pressure drop from other pressure drop terms resulting, for example, from gas compressibility and potential small temperature variations. (The simulations assume that He is an ideal gas and, for simplicity, assume adiabatic wall surfaces.) With the total pressure drop limited to 0.7 MPa in this study, however, this ambiguity is relatively insignificant.

The insensitivity of the hydrodynamic parameters to pressure is encouraging, and provides us with reasonable confidence for applying the derived closure parameters to conditions outside the range of experimental data. Similar investigations to examine the effect of pressure on flow resistance parameters in radial flow, and more importantly under oscillatory flow conditions, are recommended. We also recognize that the applicability of these parameters to cryogenic conditions needs experimental confirmation.

CONCLUSIONS

The effect of average pressure on the porous media hydrodynamic closure relations relevant to steady axial flow through four regenerator fillers was experimentally investigated. Room temperature helium was the working fluid, and the tested regenerator samples included stacked screens of stainless steel 325 mesh and stainless steel 400 mesh, screens of stainless steel 400 mesh stacked and sintered together and a stainless steel metal foam. To analyze the data, the test section and its vicinity were modeled as a porous structure using the Fluent CFD code, and the model porous media hydrodynamic parameters were iteratively adjusted to match the model predictions to the experimental results. The axial viscous and inertial resistances related to the Darcy permeability and Forchheimer's inertial coefficient, respectively, were calculated, and were found to be insensitive to the test section average pressure, provided that the maximum pressure drop through the porous sample was limited to about 0.7 MPa (100 psi).

Table 2. Sample hydrodynamic parameters.

Porous Media	Viscous Resistance $1/m^2$	Inertial Resistance 1/m	Darcy Permeability m^2	Forchheimer's Coefficient ---
325 SS Mesh	2.35E+10	47000	2.067E-11	0.316
400 SS Mesh	2.77E+10	73000	1.753E-11	0.452
400 SS (Sintered) Mesh	8.00E+10	205000	4.751E-12	0.953
SS Foam	2.65E+10	99000	1.161E-11	0.988

REFERENCES

1. Cha, J.S., “Hydrodynamic Parameters of Micro Porous Media for Steady and Oscillatory Flow: Application to Cryocooler Regenerators,” Doctoral Thesis, Georgia Institute of Technology, Atlanta, GA (2007).
2. Hsu, C., *Handbook of Porous Media* (2nd Ed.), Taylor and Francis Group, (2005), pp. 40-62.
3. Clearman, W.M., "Measurement and Correlation of Directional Permeability and Forchheimer’s Coefficient of Micro Porous Structures Used in Pulse-Tube Cryocoolers," Masters Thesis, Georgia Institute of Technology, Atlanta, GA (2007).
4. Cha, J.S., Ghiaasiaan, S.M., Desai, P.V., Harvey, J.P., and Kirkconnell, C.S., “Multi-Dimensional Effects in Pulse Tube Refrigerator,” *Cryogenics*, Vol. 46 (2006), pp. 658-665.
5. FLUENT 6 Users Manual, Fluent Inc., 2003.
6. Wilson, L., Narasimhan, A., Venkateshan, S.P., “Permeability and Form Coefficient Measurement of Porous Inserts With Non-Darcy Model Using Non-Plug Flow Experiments,” *Journal of Fluids Engineering*, Vol. 128 ASME (May 2006), pp. 638-642.